DOE Award # **DE-FG02-07ER46477**

Montana State University

Title: **Multicomponent Protein Cage Architectures for Photocatalysis**

Principal Investigator: **Professor Trevor Douglas**
Montana State University

Co-Investigators: **Professor Bern Kohler**
Montana State University

Period Covered: **9/01/2011 - 8/31/2014**

Report Date: **11/20/2014**

This report has no patentable or protected data

Executive Summary

The central focus of the work performed under this award has been to develop the bacteriophage P22 viral capsid as a vehicle for the encapsulation of catalyticaly active cargo materials and study their utility towards economic energy harvesting systems. We have demonstrated that the capsid of the bacteriophage P22 can be used to genetically program the assembly and encapsulation of a range of inorganic nanoparticles and protein cargoes. The P22 capsid uses a scaffold protein (SP) to direct the assembly of its coat protein (CP) into icosahedral capsids. By creating a genetic fusion of a desired cargo enzyme or a small peptide that can act as a nucleation site for subsequent NP growth, we have demonstrated the co-assembly of these SP-fusions and CP into stable "nano-reactors". The cargo is sequestered inside the engineered capsid and can either be used directly as a nanocatalyst or for the nucleation and growth of inorganic or organic nanoparticles or polymers. The synthetic cargos (NP or polymers) were shown to have photocatalytic activity. The time dependent photophysics of a select few of these systems were studied to determine the underlying mechanisms and efficiency of light harversting. Enzyme cargos encapsulated within the P22were thermally activated catalysts and their kinetic behavior was characterized. During the course of this work we have demonstrated that the method is a robust means to harness biology for materials applications and have initiated work into assembling the P22 nanoreactors into hierarchically ordered materials. The successful implementation of the work performed under this DOE grant provides us with a great deal of knowledge and a library of components to go forward towards the development of bioinspired catalytic materials for energy harvesting.

Comparison of the actual accomplishments with the goals and objectives of the project.

The project has been very successful and we have demonstrated that the aims originally proposed could be demonstrated. The Aims of the Project were 1) to encapsulate Materials on the interior of the P22 Protein Cage 2) modification to the exterior of the P22 cage 3) to uses alternative architectures based on symmetry broken P22 capsids and 4) to probing the spectroscopic characteristics of P22 templated materials.

We have clearly demonstrated the directed encapsulation of both inorganic and organic-based photo catalytically active materials within the P22 cage. We successfully identified domains on the P22 capsid which are exposed to the exterior environment and demonstrated that we could use this to functionally manipulated the capsid. In addition modification of a small protein that binds to the exterior of P22 was modified to affect directed hierarchical assembly of the P22 capsids into bulk-like materials. We successfully demonstrated that we could modify symmetry-broken P22 capsids with the portal incorporated at one 5-fold vertex using the incorporation of non-natural amino acids at surface exposed residues. The photoinduced electron transfer between ruthenium(II)-cobalt(III)centers from a series of polymeric components, that could be incorporated into the P22, were probed. In addition, the photophysics of small inorganic nanoclusters of Ce-oxide revealed that nanoparticles of cerium oxide form spontaneously due to cerium(IV) hydrolysis. Femtosecond transient absorption experiments revealed dynamics consistent with electron-hole pair recombination. Lastly, initial work on the assembly of P22 capsids into ordered long range arrays demonstrated that this could be achieved through the use of a designed linker that effectively crosslinks the individual P22 capsids into a bulk material.

ACCOMPLISHMENTS

1) Directed Encapsulation of Materials on the Interior of the P22 Protein Cage (Aim 1) Montana State University (Douglas)

We have demonstrated the directed encapsulation of a range of enzymes with relevance to energy conversion and utilization. The C-terminal region of the scaffold protein is required for the templated assembly of the P22 capsid and the N-terminal region of the scaffold protein can be truncated or fused to other proteins without loss of assembly. This results in sequestration of the fused cargo on the interior of the capsid at high packing density.

- We have explored the effects of molecular co-confinement and inter-protein communication using green fluorescent protein (GFP) and mCherry fluorescent protein co-encapsulated inside P22. Efficient energy transfer between the donor (GFP) and acceptor (mCherry) was observed and varying the linker length between the GFP and mCherry had no effect on the FRET efficiency but unencapsulated controls of this donor-acceptor pair showed the expected distance dependence. These results strongly suggest that co-encapsulation (at high density) of interacting macromolecules within the P22 results in enforced communication between the active cargo molecules.
- We have demonstrated the co-encapsulation of two enzymes that share a substrate-product relationship (ie the product of the first enzyme is the substrate fro the second enzyme). Thus we encapsulated a glucosidase enzyme (CelB), which cleaves lactose into glucose and galactose, together with a glucokinase (GluK) and a galactokinase (GalK) has been investigated. This coupled series of reactions represents a portion of a synthetic metabolic pathway for disaccharide utilization. This highlights the potential of this approach for directed synthesis of designed cascade reactions for energy applications. Synthesis is done at the level of molecular biology and these unique P22 nanoreactors self assemble in *E. coli* in a highly reproducible manner. The published results demonstrated that although these enzymes are encapsulated in high density within the P22 capsid there is no evidence of an overall enhancement of the rate of the coupled reaction as compared to separately encapsulated enzymes. This is demonstrates that the enzymes are not diffusion limited and the experimental results were validated by a mathematical model developed to understand the complex coupled kinetics. Importantly this work demonstrates that it is not necessary to co-encapsulate all enzymes in a synthetic pathway into a single capsid and this suggests a way forward for the construction of complex coupled enzymatic systems in materials applications.
- A similar approach using the SP fusion has been successfully applied to the co-encapsulation of the two subunits of the *E. coli* [NiFe] hydrogenase (Hyda and HydB). The resulting P22 nanoreactors self assemble in *E. coli*, package up to 200 copies of the heterodimeric enzyme in each P22 capsid and are air stable (**Fig. 1**). The enzyme very efficiently catalyzes the formation of H_2 (measured by gas chromatography) using reduced methyl viologen as a redox mediator.

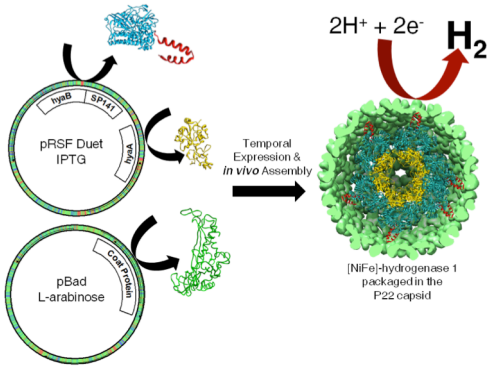

Fig. 1. Co-expression of the subunits hyaA and hyaB as SP fusion proteins, together with CP results in encapsulation of [NiFe] hydrogenase, which is active for H_2 production.

- We have shown that modification of the P22 capsid interior with small molecule initiators can be used to synthesize functional polymers in a three-dimensional polyaminoethylacrylate (AEMA) network, constrained within the capsid architecture. This is a promising strategy to take full advantage of the interior volume. A cysteine mutant S39C was used to anchor the initiator for atom transfer radical polymerization (ATRP) and this approach has been used to incorporate monomers of $Ru(phen)_3^{2+}$ in which each phenanthroline carries an acrylamide functionality and thus can act as a crosslinking agent between polymer strands. The incorporated $Ru(phen)_3^{2+}$ -AEMA polymer is photoactive and, under visible illumination, the P22-AEMA-$Ru(phen)_3^{2+}$ composite efficiently

catalyzes the reduction of methyl viologen using EDTA (45mM) or ethanol (10%) as a sacrificial reductant. We have constructed a P22 material which is an efficient photocatalyst for generating the redox mediator (reduced methyl viologen) required for the hydrogenase enzyme mentioned in the previous bullet. This suggests a way forward in the construction of new materials based on P22 where both enzymatic (hydrogenase) and light harvesting (polyAEMA-$Ru(phen)_3$) P22 particles could be assembled into long range materials.

- By combining both enzymatic and small molecule catalysts together, new hybrid biological-synthetic catalytic materials have been produced incorporating the best of both systems. We have combined and covalently coupled $Cp^*Rh(phen)Cl^+$ and the enzyme alcohol dehydrogenase (AdhD) into the P22 capsid, which co-localizes the catalysts and enzyme in close proximity (**Fig. 2**). The Cp*Rh(phen)Cl catalyst reduces NAD+ to NADH using formate as a sacrificial reductant while the AdhD enzyme reduces 2-hydroxybutanone (acetoin) to 2,3-butandiol using NADH. The reaction kinetics of this coupled co-catalyst system can be tuned to generate a steady-state turnover. The importance of this lies in the need to drive enzymatic reductions using NADH, which is an expensive molecule to produce. However, by incorporating the small molecule organometallic catalyst we can recycle NADH, for use by the enzyme, through a coupled reaction using a sacrificial reductant such as formate.

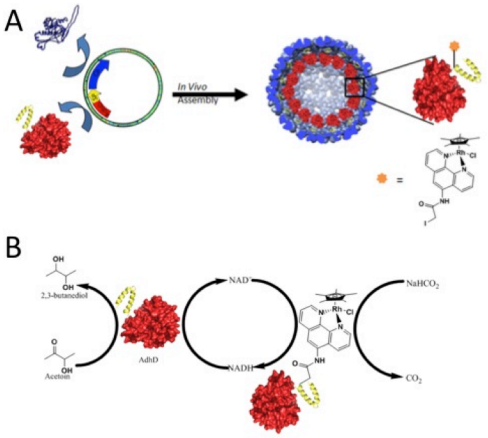

Fig. 2. A. Self-assembly of the P22-AdhD nanoreactor and attachment of the Cp*Rh(phen)Cl. B. The reaction catalyzed by AdhD oxidizes NADH and converts acetoin into 2,3-butandiol. The reaction catalyzed by the Cp*Rh reduces NAD+ using formate as the reductant.

2) Modification of the Exterior Surface of P22 Protein Cages. (Aim 2) Montana State University (Douglas)

We have demonstrated the controlled assembly of protein cages using modifications to the capsid exterior. Individual P22 capsids fused with complementary coiled-coil peptides (E-coil and K-coil) assemble to form larger structures only when P22 with E-coil and P22 with K-coil are mixed together. Structural analysis of these hierarchically assembled materials is underway in collaboration with Dr. Masafumi Fukuto and Dr. Lin Yang at Brookhaven National Laboratory by small angle X-ray scattering. Data collection on the assembled structures using the SAXS facility at beamline X9 at NSLS (**Fig. 3**) indicates a degree of long-range order in the assembly composed of protein cages.

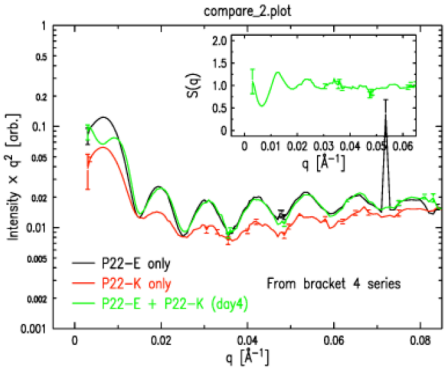

Fig. 3. SAXS of P22-E coil (black), P22-K coil (Red) and assembly of P22-E coil and P22-K coil (Green). Ratio between the assembled P22 and P22-E coil (inset) represents structure factor from the assembly. The peak at q=0.0127 corresponds to close-packing of P22 capsids.

- Dec- assembly. A small (15kDa) decoration protein (Dec) has been shown (cryo TEM) to bind as a trimer to the P22 capsid orientated with the C-terminus directed away from the capsid surface. We have shown that we can modify the C-terminus of Dec without significantly affecting the binding to P22. Using the Dec, we have constructed two different linker proteins capable of binding to P22 capsids and affecting the crosslinking between capsids with different multivalency and geometries. In one case a dimer of the Dec

trimer was constructed by introducing a cysteine at the C-terminus of Dec and oxidizing this to make an end-to-end dimer. This generates a ditopic protein that can non-covalently link P22 capsids into an extended material. Also, we have constructed a fusion between the C-terminus of the Dec protein and the N-terminus of a small cage protein (Dps), which assembles into a tetrahedral cage like protein. Thus the Dec trimer is commensurate with the 3-fold symmetry axis odf the Dps protein making a connector with tetrahedral symmetry and the potential to link 4 P22 capsids together. We have shown, using these constructs, that we can make long range arrays of P22 and demonstrated/monitored this using QCM-D to make layer-by-layer assemblies (**Fig 4**) with alternating P22 and Dec-construct layers.

• Dendrimer mediated assembly. The condensation of P22 with either PEG-6000 or PAMAM dendrimer G6.0 results in ordered assembly and has been probed using solution light scattering, synchrotron based small angle X-ray scattering (SAXS), and transmission electron microscopy.

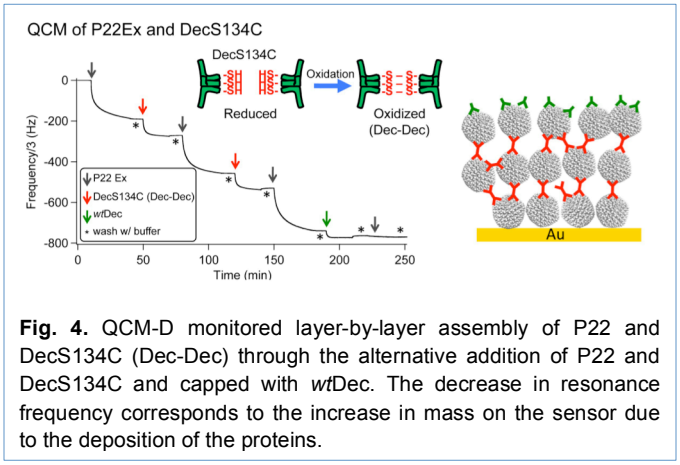

Fig. 4. QCM-D monitored layer-by-layer assembly of P22 and DecS134C (Dec-Dec) through the alternative addition of P22 and DecS134C and capped with *wt*Dec. The decrease in resonance frequency corresponds to the increase in mass on the sensor due to the deposition of the proteins.

3) Using Alternative Architectures Based on Symmetry Broken P22 Capsids, with Portal Complex, as Templates (Aim 3) Montana State University (Douglas)

To incorporate asymmetry into the P22 encapsulation system, the naturally occurring P22 portal protein, which occurs at only one of the five-fold vertices, has been integrated into a heterologous P22 expression system. Single amino acids on the portal protein, exposed to the exterior of the capsid (T377, N380) have been substituted for either a cysteine or a methionine (**Fig. 5**). Using the reassignment of the met codon for, a methionine analog (azidohomoalanine, AHA) was incorporated into the N380M portal protein mutant, which provides a reactive azide moiety, which reacts via a Cu(I) catalyzed click reaction with an alkyne-fluorescein for site selective labeling (Fig. 4).

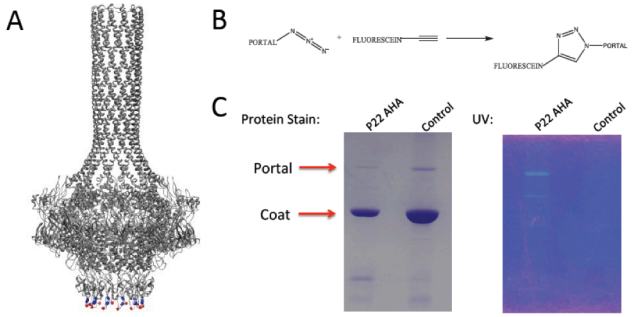

Fig. 5. (A) Structure (PDB: 3JL5) of the P22 portal protein with T377C mutation (blue) and N380M (red). (b) Reaction of fluorescein-alkyne with the azide on the portal protein. (C) Left, denaturing SDS-PAGE gel with coat and portal proteins (coomassie stain). Right, the same gel illuminated by UV showing specific fluorescein labeling of the azide containing portal (P22-AHA lane).

4) Probing the Spectroscopic Characteristics of P22 Templated Materials (Aim 4) Montana State University (Kohler)

Photoinduced electron transfer in ruthenium(II)-cobalt(III) clusters. The excited-state dynamics of a Ruthenium(II)-Cobalt(III) multi-metal complex (**Fig. 6**) was studied using ultrafast transient absorption (TA) and time-correlated single photon counting (TCSPC) techniques. This complex is a prototype for macromolecular light-sensitized catalysts that are easily synthesized via "click" chemistry. The focus of the work was on understanding how the triazole linker mediates electron transfer (ET) between metal centers in a

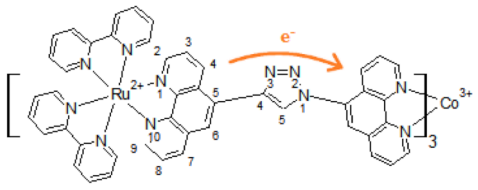

Fig. 6. The Ruthenium(II)-Cobalt(III) complex.

metallopolymer. There is debate currently about whether the triazole linker aids or hinders photoinduced ET in donor-acceptor dyads.

The emission quantum yield of the complex in Fig. 1 is 80% as large as for the separate, monometallic ruthenium(II) complex. Time-resolved emission experiments indicate that ET occurs at a slow rate of 6.7×10^6 s^{-1} in agreement with previously measured rates of between $(0.4 – 1.0) \times 10^7$ s^{-1} for dyads in which a ruthenium(II) polypyridyl donor is linked at the 4-position of triazole to an acceptor group. Rates increase approximately tenfold when the donor complex is attached to the N1 atom of the triazole, but these rates are still too low for metal-to-metal ET to compete efficiently with radiative and alternative nonradiative decay channels. These results suggest that triazole bridges have drawbacks for ET, but may exhibit higher rates of hole transport. Our work also suggests that it would be valuable to explore effects due to 4- vs. 5-substitution on the 1,10-phenanthroline ligand. It has been shown that extended conjugation in 4-substituted phenanthroline ligands strongly perturbs emission spectra and lifetimes of the ^{3}MLCT states of ruthenium(II) sensitizers, while substitution at other positions leads to emission spectra and lifetimes that are hardly altered compared to the unmodified complex.

A comprehensive study was completed of excited-state localization in the series of mixed-ligand complexes $[Ru(bpy)_n(phen)_{3-n}]^{2+}$ (n = 0,1,2,3), where bpy is 2,2'-bipyridine and phen is 1,10-phenanthroline. Although there is growing consensus that ^{3}MLCT states of ruthenium(II) polypyridyl complexes are localized on a single ligand—even in homoleptic complexes like $[Ru(bpy)_3]^{2+}$—there is still considerable uncertainty about how quickly an excitation on one ligand can hop to another. Understanding the factors that govern interligand electron transfer (or exciton hopping) are critically important for designing photosensitizers that optimally direct a photoexcited electron to a desired ligand.

Although the bpy- and phen-localized ^{3}MLCT states in the $[Ru(bpy)_n(phen)_{3-n}]^{2+}$ complexes have similar energies and steady-state emission spectra, pronounced differences in their excited-state absorption spectra made it possible to determine excited state populations using magic-angle TA spectroscopy. The results show that the initial excited state rapidly hops between all three ligands at times < 1 ps and the excited state is equally likely to be found on any of the three ligands. Over the next several tens of ps, the excited state population progressively shifts to favor localization on bpy. A model in which ILET rates depend on excess vibrational energy explains these observations. For $[Ru(bpy)(phen)_2]^{2+}$, the initial Franck-Condon excited state has energy in excess of that required to pass over the energy barriers between the different localized states, and ILET proceeds in hundreds of femtoseconds. As vibrational cooling dissipates this excess energy into the surroundings, ILET changes to a weakly activated process, and a Boltzmann distribution of localized ^{3}MLCT states is reached on the time scale of vibrational cooling. Because of the small splitting between bpy- and phen-localized excited states (D*E* = 150 – 310 cm^{-1}), ILET is estimated to occur with a time constant of approximately 10 ps, a value that is much shorter than the luminescent lifetime consistent with the observation of a single decay time in time-resolved emission experiments.

In 2014, visible pump/mid-IR probe TA experiments made it possible to more readily separate vibrational cooling from population dynamics. Results show an increase in a vibrational marker band assigned to reduced bpy over the 10 ps time scale, while no change is observed in this band in the case of $[Ru(bpy)_3]^{2+}$.

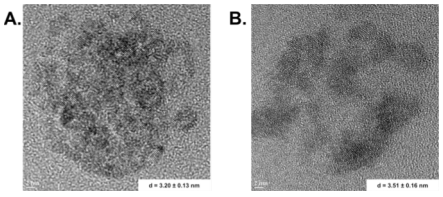

Fig. 7. HRTEM images of P22 stuffed shells containing either the T141303 scaffolding construct (A), or the S141303 scaffolding construct (B). The particles were incubated with TiBALDH for 24 h before imaging. The observed d-spacing in (A) corresponds to the (110) plane of rutile and the d-spacing in (B) corresponds to the (101) of anatase.

5) Internal TiO_2 Mineralization of P22 (Aim 5) University of Alabama and Montana State University (Douglas)
We have extended our studies of internal TiO_2 mineralization

of P22 to include an additional peptide sequence reported to nucleate the crystallization of the anatase form, characterization of the crystallinity and size of the TiO_2 nanoparticles, and a demonstration of photo-catalytic activity.

- Incorporating peptides for internal mineralization: We have constructed a P22 particle in which the peptide sequence CHKKPSKSC was fused to the N-terminus of the central and C-terminal region (residues 141-303) of P22 scaffolding protein (designated T141-303). This peptide was chosen because it had been reported to nucleate the formation of TiO_2 from TiBALDH precursor. Over the past year we have generated an additional construct carrying the sequence RKLPDAPGMHTW, which has been reported to nucleate the formation of anatase TiO_2 (designated S141-303). A robust strategy for controlling the amount of fusion protein inside the protein cages by re-entry has been developed and employed insuring high occupancy.
- Characterization of TiO_2 nanoparticles: TiO_2 nanoparticles were formed by incubation of P22 shells loaded with scaffolding fusion proteins T141-303 and S141-303 with TiBALDH under room temperature conditions. Unstained transmission electron microscopy (TEM) and dark field STEM suggested the formation of electron dense clusters contained within the particles. Dynamic light scattering (DLS) and analytical ultracentrifugation (AU) demonstrated that the outer diameter of the protein cage was unchanged following treatment. High resolution TEM (HRTEM) was employed to ascertain whether the electron dense clusters were crystalline TiO_2 (**Fig. 7**). For both the T141-303 construct and the S141-303 construct distinct lattice fringes were observed. The measured d-spacing in the T141-303 particles was 3.2 ± 0.16 Å, which corresponds to the 110 plane of rutile TiO_2 (3.19 Å), while the d-spacing in the S141-303 particle was 3.51 ± 0.16 Å, which corresponded to the 101 plane of anatase TiO_2 (3.51 Å). The size of the particles within the protein cage was estimated by dissociation of the protein shell followed by sedimentation velocity AU of the TiO_2 particles**.** The particles sediment with a narrow distribution of s-values which can be used to estimate the diameter of the particles as ~ 4 nm. This diameter is roughly 10% of the internal diameter of the protein cage and suggests that multiple nucleation events are occurring within a given protein cage.

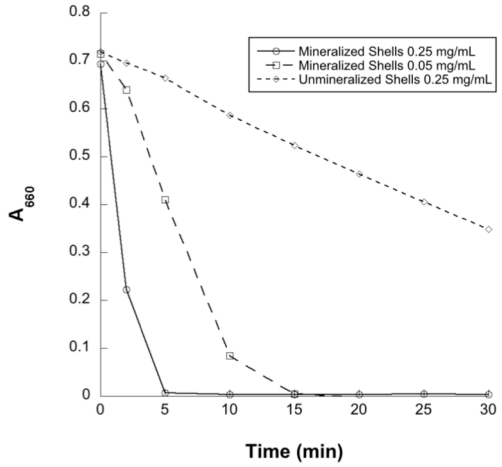

Fig. 8. Photoreduction of methylene blue in the presence of 0.25 mg/mL (solid line), 0.05 mg/mL (dashed line), or 0.25 mg/mL unmineralized stuffed shells (dotted line). The $t_{1/2}$ values for each of these samples is approximately 2.5 min, 6 min, and 30 min, respectively.

- Photoactivity of TiO_2 containing particles: The photoactivity of the TiO_2 containing particles was evaluated by measuring the photo-reduction of methylene blue (MB) upon illumination with a Xe arc lamp (**Fig. 8**). Photoreduction of MB results in a decrease in absorbance at 660 nm. Unmineralized shells have a $t_{1/2}$ of photoreduction of approximately 30 min, whereas the $t_{1/2}$ for photoreduction when the same quantity of mineralized shells is included drops to 2.5 min. As expected, smaller quantities of mineralized particles result in intermediate reaction half-lives.

Photophysics of metal oxide nanoparticles and precursor complexes. A project aim was to investigate the photocatalytic properties of functionalized metal oxide nanoparticles prepared using P22 synthetic techniques. Cerium oxide and iron oxide nanoparticles (NPs) were studied in aqueous solution by femtosecond TA spectroscopy. Cerium oxide is a redox-agile material of growing interest as a component

of solid oxide fuel cells and as a mimic of superoxide dismutase that inhibits cellular damage by reactive oxygen species in vivo. Iron oxides are attractive building blocks for solar energy conversion because of their low cost.

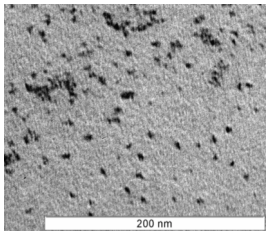

Fig. 9. Transmission electron microscope (TEM) image of one-week-old solution of 1 mg CAN in 5 mL of H_2O showing cerium oxide nanoparticles

An important discovery was the observation of spontaneous cerium oxide NP formation from aqueous solutions of cerium(IV) ammonium nitrate (CAN) above pH ~0.5. The NPs form spontaneously due to cerium(IV) hydrolysis. NP growth kinetics could be conveniently monitored by changes in the UV/vis absorption spectra that occur over a period of a few minutes and that reflect a strong increase in O_{2p} to Ce_{4f} charge transfer absorption upon NP formation. The growth proceeds by second-order kinetics and displays a large solvent kinetic isotope effect (k_{H_2O} / k_{D_2O}). At pH 2, 2–3 nm diameter NPs are formed (**Fig. 9**).

The presence of cerium oxide NPs was confirmed by femtosecond TA experiments that revealed dynamics consistent with electron-hole pair recombination (**Fig. 10**). In follow-on studies, the rates of electron-hole recombination are being measured and compared with dynamics in better-studied TiO_2 NPs.

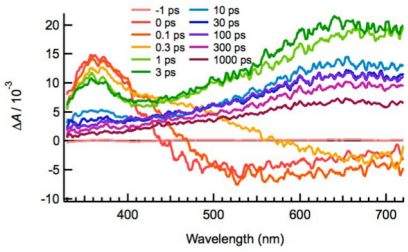

Fig. 10. TA spectra showing electron-hole recombination in CeO_2 NPs.

PRODUCTS

Publications *(Acknowledgement sections are included).*

1. Alison O'Neil, Peter E. Prevelige, Gautam Basu, Trevor Douglas, "Co-Confinement of Fluorescent Proteins: Spatially Enforced Interactions of GFP and mCherry Encapsulated Within the P22 Capsid" *Biomacomolecules* (2012) 13, 3902-3907.

This research was supported by the U.S. Department of Energy, Office of Basic Energy Sciences, Division of Materials Science and Engineering DE-FG02-07ER46477.

2. Janice Lucon, Shefah Qazi, Masaki Uchida, Greg Bledwell, Ben LaFrance, Peter Prevelige, and Trevor Douglas "Use of the interior cavity of the P22 capsid for site-specific initiation of atom-transfer radical polymerization with high-density cargo loading" *Nature Chemistry* (2012) 4, 781-788. [Cover]

This research was supported in part by grants from the National Institutes of Health (R01- EB012027), the National Science Foundation (CBET-0709358) and a National Science Foundation Graduate Research Fellowship (J.L.). P.E.P. and G.J.B. were supported by the US Department of Energy, Office of Basic Energy Sciences, Division of Materials Sciences and Engineering (DE-FG02-08ER46537).

3. Janice Lucon, Ethan Edwards, Shefah Qasi, Masaki Uchida, Trevor Douglas "Atom Transfer Radical Polymerization on the Interior of the P22 Capsid and Incorporation of Photocatalytic Monomer Crosslinks" *Eur. Polymer Journal* (2013), 49, 2976-2985. [Cover]

This research was supported by the U.S. Department of Energy, Office of Basic Energy Sciences, Division of Materials Science and Engineering DE-FG02-07ER46477, and J.L. was supported on a National Science Foundation Graduate Research Fellowship.

4. Dustin P. Patterson, Benjamin Schwarz, Ryan Waters, Tomas Gedeon, Trevor Douglas "Encapsulation of an Enzyme Cascade Within the Bacteriophage P22 Virus-Like Particle" *ACS Chemical Biology (*2014) 9, 359–365. *DOI:10.1021/cb300388w*

The experimental work was supported by grants from U.S. Department of Energy, Office of Basic Energy Sciences, Division of Materials Science and Engineering DE-FG02- 07ER46477 (coupled enzyme catalysis and the work on the kinases) and the National Science Foundation BMAT-1104876 (CelB component of the research).

5. Dustin Patterson, Ethan Edwards, and Trevor Douglas "Hybrid Nanoreactors: Coupling Enzymes and Small-Molecule Catalysts within Virus-Like Particles" *Israel J. Chem* (2014) *DOI: 10.1002/ijch.201400092*.

This research was supported by the U.S. Department of Energy, Office of Basic Energy Sciences, Division of Materials Science and Engineering DE-FG02-07ER46477.

6. Paul Jordan, Kendall Saboda, Gautam Basu, Megan Thielges, Trevor Douglas "Engineering a Virus for Hydrogen Production" Nature Chemistry *manuscript in revision*

This research was supported by a grant from US Department of Energy, Office of Basic Energy Sciences, Division of Materials Sciences and Engineering (DE-FG02-07ER46477).

7. Dustin Patterson, Ethan Edwards, and Trevor Douglas "Hybrid Nanoreactors: Coupling Enzymes and Small-Molecule Catalysts within Virus-Like Particles" *Israel J. Chem* (2014) *DOI: 10.1002/ijch.201400092*.

This research was supported by the U.S. Department of Energy, Office of Basic Energy Sciences, Division of Materials Science and Engineering DE-FG02-07ER46477

8. Amy Servid, Paul Jordan, Alison O'Neil, Peter Prevelige, Trevor Douglas "Location of the Bacteriophage P22 Coat Protein C-terminus Provides Opportunities for the Design of Capsid Based Materials" *Biomacromolecules* (2013) 14, 2989–2995.

This work was supported in part by grants from the National Institutes of Health, NIBIB R01-EB012027 (design and construction of the C-terminal constructs), and the U.S. Department of Energy, Offi ce of Basic Energy Sciences, Division of Materials Science and Engineering, DE-FG02-07ER46477 (hierarchical assembly of E-coil and K-coil constructs).

9. Masaki Uchida, Benjamin LaFrance, Chris C. Broomell, Peter E. Prevelige, Trevor Douglas "Higher order assembly of virus-like particles (VLP) mediated by multi-valent protein linkers" *Small* (2014) *accepted – in press.*

Characterization of P22 assembly into higher order assemblies was supported by a grant from US Department of Energy, Office of Basic Energy Sciences, Division of Materials Sciences and Engineering (DE-FG02-07ER46477).

10. Gregory J. Bedwell, Ziyou Zhou, Masaki Uchida, Trevor Douglas, Arunava Gupta, and Peter E. Prevelige, Jr., "Biotemplated synthesis and characterization of photoactive TiO_2 nanoparticles inside a P22-derived Protein Cage nanoarchitecture", *submitted Biomacromolecules (2014).*

Manuscripts in preparation:

1. Charles Stark, Wolfgang Schreier, Janice Lucon, Ethan Edwards, Trevor Douglas, and Bern Kohler, Excited-state localization in ruthenium mixed-ligand complexes studied by femtosecond transient absorption spectroscopy, *manuscript in preparation*.
2. Wolfgang Schreier, Charles Stark, Janice Lucon, Ethan Edwards, Trevor Douglas, and Bern Kohler, Excited-state dynamics of ruthenium(II)-cobalt(III) metallodendrimers assembled by click chemistry, *manuscript in preparation*.
3. Pettinger, N.; Chen, J.; Theiste, P.; Kohler, B. Cerium Oxide Nanoparticles from Ceric Ammonium Nitrate: Just Add Water, *J. Phys. Chem. Lett.*, *to be submitted*.

Patents

Nothing to report

3. SUPPORTED PERSONNEL

	Calendar Months of Support		
	Year 1	Year 2	Year 3
Trevor Douglas (PI)	6	-	1.0
Bern Kohler (co-PI)	0.5	0.5	0.5
Ethan Edwards (graduate student)		11	11
Paul Jordan (graduate student)	8	2	10
Kimberly McCoy (graduate student)	-	-	8
Charles Stark (graduate student)	12	12	12
Rebecca Danforth (graduate student)	-	3	12
Peder Theiste (graduate student)	-	-	3
Natasha Pettinger (undergraduate student)	-	3	3
Ben LaFrance (undergraduate student)	-	1	3
Kendal Saboda (undergraduate student)	-	8	5
Heini Miettinen-Granger (technician)	-	2	12
Carmen Eibs (technician)	-	-	4
Dustin Patterson (post-doc)	8	12	-
Benjamin Schwarz (graduate student)	-	5	-
Masaki Uchida (post-doc)	-	-	2
Josh Sinrud (undergraduate student)	-	-	4